AIAA 80-0693R

Cyclic Plasticity and Fatigue of Structural Components

I. Kalev*
National Research Council/NASA Dryden Flight Research Center, Edwards, Calif.

An analytical approach for low-cycle fatigue life prediction is presented. It accounts for both life to crack initiation and crack growth rate due to cyclic plasticity. The approach combines a cyclic plasticity model with the finite-element method and damage accumulation criteria for ductile metals. The cyclic plasticity model is based on the concept of the combination of several yield surfaces. The surfaces are related to the material uniaxial stress-strain curve idealized by piecewise linear segments. The damage criterion for crack initiation is based on plastic strain Coffin-Manson formula modified for both mean stress variation effect and multiaxial varying stress-strain field. Crack growth rate is approximated by the inverse damage accumulation gradient in front of the crack tip. Crack growth retardation effects due to plasticity stress redistribution and compressive residual stresses are included. This approach requires testing data of only smooth specimens under constant strain amplitudes. Illustrative examples of a stiffened panel on an aircraft wing are presented.

Introduction

FATIGUE crack initiation and crack growth rate up to complete failure of aircraft ductile metals are mainly governed by the plasticity process.

In case the plasticity zone developed in structural component is very small, a simplified linear elastic analysis can be employed. Most of the widely used linear elastic approaches are based on the stress amplitude. The classical S-N curves[1] have been applied for crack initiation prediction, and the fracture mechanics net section stress-intensity range has been related to crack growth rate.[2,3] However, if the plasticity zone is large the stress-intensity loses its physical meaning because of stress redistributions and developed residual stresses.

In order to account for the plasticity effects, plastic strain amplitude should be incorporated into the fatigue criterion. Numerous analyses[4-6] have employed the well-known Coffin-Manson plastic strain life criterion[7] in conjunction with the simplified Neuber formula[8] for life to crack initiation prediction. However, this simplified approach is suitable only when the stress-strain state is uniaxial and localized in the notch region. The J integral method has been applied for inclusion of plasticity effects on residual strength of cracked structure[9] and on crack growth process.[10] The J integral is related to the stress-intensity factor in elastic range, and it also retains its physical meaning in plastic range. However, as it is based on the path-independent deformation theory of plasticity, it is restricted to proportionally and monotonically increased loading as in the case for residual strength calculation without the unloading and reversed plastic loading which occur during the crack growth process.

This paper presents an analytical approach for inclusion cyclic plasticity effects on prediction of life to crack initiation and crack growth rate up to complete structural failure. This analysis is required to insure integrity of aircraft structures. Cyclic plasticity could be developed under an applied load variation which is not necessarily of a fully cyclic type. That is because of the material Bauschinger's phenomenon which leads to early plastic reloading after unloading. The present approach is composed of three analytical components and requires three groups of input data in order to compute the number of reversals to crack initiation, the crack growth rate and orientation, and the total reversals to failure. A general flow diagram of the approach is shown in Fig. 1. The first item in Fig. 1 is a mathematical model of the specific uncracked or cracked component and the numerical procedures for determination of static and dynamic stress-strain distribution. For such determination, it is widely acknowledged that the finite-element method is the most suitable, due to both its versatility regarding real complex geometries and the good correlation with testing data that can be achieved. The second item is a cyclic plasticity model for determination of the large material strains at each cycle. The third item is the damage accumulation criteria which indicate life to crack initiation and crack growth rate. Crack growth retardation effects due to stress redistributions and compressive residual stresses are included. As shown in Fig. 1, the input data include the applied loading spectrum, the material uniaxial cyclic steady-state stress-strain curve, and the material uniaxial constant strain amplitude fatigue parameters. The material fatigue parameters are a Coffin-Manson exponent derived from unnotched specimens, an exponent which relates stress amplitude to plastic strain amplitude, and an exponent which indicates the rate of mean stress relaxation due to cyclic plasticity.

Cyclic Plasticity Model

A suitable plasticity model for determination of stress-strain variation during plastic loading, unloading, and reversed plastic loading is essential for low-cycle fatigue damage accumulation. In this study the plasticity model is based on the classical incremental time-independent and rate-independent plastic flow theory for initial isotropic materials.

Incremental plastic flow theory requires definition of an initial yield surface, a plastic flow law, and a hardening rule. For ductile metals, the von Mises criterion is widely acknowledged as an appropriate representative of initial yield surface. Its associated plastic flow law predicts that the plastic strain increment is normal to the yield surface at the current stress point. In addition, it is assumed that the elastic strain increment is much smaller than the plastic strain increment, and that both are independently and linearly related to the stress increment. The present hardening rule is based on the combined translations in stress space of several yield surfaces. Each yield surface $f^{(i)}$, $i=1,2,\ldots$, relates one of the piecewise linear segments idealizing the material uniaxial stress-strain curve (shown in Fig. 2a) to the multiaxial stress state σ_i, $i=1,2,\ldots,9$, shown schematically in Fig. 2b. Each yield surface is defined by the von Mises criterion and is allowed to translate in stress space up to its bounding surface to which it remains connected until unloading stage. The translation rate

Presented as Paper 80-0693 at the AIAA/ASME/ASCE/AHS 21st Structures, Structural Dynamics and Materials Conference, Seattle, Wash., May 12-14, 1980; submitted May 29, 1980; revision received Dec. 24, 1980. This paper is declared a work of the U.S. Government and therefore is in the public domain.

*Research Associate. Member AIAA.

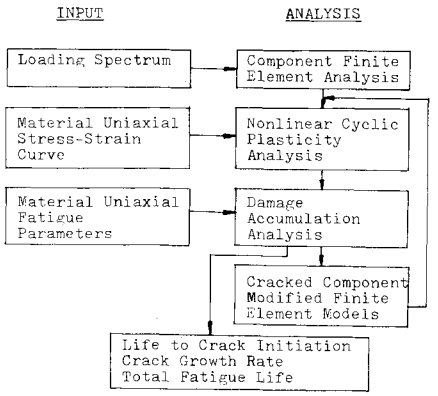

Fig. 1 Flow diagram for fatigue life prediction.

$d\alpha$ is governed by the Mroz's hardening rule.[11] The Mroz's rule is based on the inherent fulfillment of the nonintersection requirements among the yield surfaces, as depicted in Fig. 2b.

The present model assumes that the material at its uniaxial cyclic steady state obeys the Masing's postulation, i.e., the uniaxial curve is magnified after the first unloading by a factor of two, as depicted in Fig. 2a. Most metals used in aircraft obey this description. In addition, it is assumed that the material preserves in its memory the maximum von Mises stress value for an indication of the plastic reloading stage.

The cyclic plasticity room temperature stress relaxation phenomenon is not included in the present plasticity model, but this phenomenon is incorporated in the present damage criterion which is discussed later.

The mathematical expressions of the plasticity model are presented in Ref. 11.

Crack Initiation Criterion

According to the Coffin-Manson equation,[7] the constant uniaxial plastic true strain range $\Delta\epsilon^p$ per one cycle (two reversals) is related to the number of reversals to crack initiation $2N$, as follows:

$$\Delta\epsilon^p/2=\epsilon_f'(2N)^c \tag{1}$$

where c is the material low-cycle fatigue exponent and ϵ_f' is the fatigue ductility parameter which is smaller than the monotonic fracture ductility parameter ϵ_f.

Equation (1) assumes zero mean stress for each stress-strain loop. Morrow[12] suggested that the Basquin's equation which relates the constant uniaxial true stress range per cycle $\Delta\sigma$ to reversals to failure could be modified to account for the mean stress σ_m effect by reducing the fatigue strength parameter σ_f' by a factor of $(1-\sigma_m/\sigma_f)$. The quantity σ_f is the material monotonic fracture strength. The sign of σ_m is plus for tensile stress and minus for compressive stress. This leads to the following relationship

$$\Delta\sigma/2=\sigma_f'(1-\sigma_m/\sigma_f)(2N)^b \tag{2}$$

when b is the material high-cycle fatigue exponent.

The material uniaxial cyclic true stress-plastic strain relationship, based on testing data on loci of tips of steady-state loops of different fully cyclic constant plastic strain amplitudes,[13] can be approximated as follows:

$$\Delta\sigma/2=[\sigma_f'/(\epsilon_f')^{n'}](\Delta\epsilon^p/2)^{n'} \tag{3}$$

where n' is material cyclic stress-plastic strain exponent. Equation (3) leads to the assumption that $b=cn'$.

By substituting Eq. (3) into Eq. (1), rearranging, and comparing to Eq. (2), it appears that the effect of the mean stress could be included in Eq. (1) as follows:

$$(\Delta\epsilon^p/2\epsilon_f')^{1/c}(1-\sigma_m/\sigma_f)^{-1/cn'}=2N \tag{4}$$

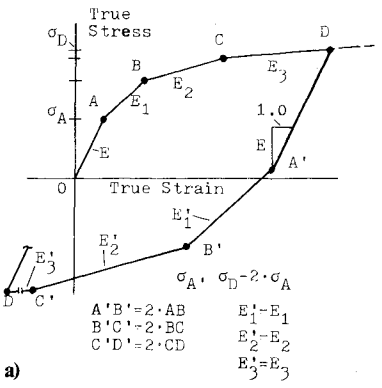

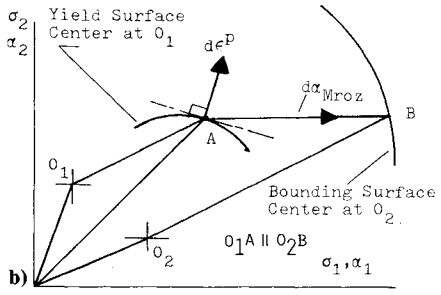

Fig. 2 Relationship between yield surfaces and material uniaxial curve. a) Uniaxial stress-strain curve idealization. b) Yield surfaces translation rule.

Now, in order to extend Eq. (4) for a multiaxial state, the quantity $\Delta\epsilon^p$ is replaced by the equivalent true plastic strain increment accumulated through each pair of reversals,

$$\int_k^{k+2} d\bar{\epsilon}^p$$

where $k+1$ and $k+2$ indicate two subsequent plastic unloadings defining the specific pair of reversals. Also, the quantity σ_m is replaced by a mean stress value $\bar{\sigma}_m$ which is the average of the values at the two unloadings. Thus,

$$(\int d\bar{\epsilon}^p/2\epsilon_f')^{1/c}(1-3\bar{\sigma}_m/\sigma_f)^{-1/cn'}=2N \tag{5}$$

and

$$d\bar{\epsilon}^p=(d\epsilon_{ij}^p d\epsilon_{ij}^p)^{1/2} \tag{6}$$

when $d\epsilon_{ij}^p$ ($i,j=1,2,3$ in tensor notation) is plastic strain increment, and

$$\bar{\sigma}_m=0.5[(\sigma_{ii}/3)_{\text{unloading }k+1}+(\sigma_{ii}/3)_{\text{unloading }k+2}] \tag{7}$$

when σ_{ii} ($i=1,2,3$ in tensor notation) is the stress component at one of the two subsequent plastic unloadings. The quantity $\bar{\sigma}_m$ represents the effect of tensile vs compressive stresses. If the reversal loading results in a symmetric stress variation, i.e., $\sigma_{ii,\max}=\sigma_{ii,\min}$, then $\bar{\sigma}_m=0$.

Equation (5) indicates that crack initiation occurs after $2N$ constant amplitude reversals. Now, if the accumulated damage D is defined as $1/(2N)$, then for various size of reversals it can be expressed mathematically as follows:

$$D=\sum_1^{2N}\left(\frac{\int d\bar{\epsilon}^p}{2\epsilon_f'}\right)^{-1/c}\left(1-\frac{3\bar{\sigma}_m}{\sigma_f}\right)^{1/cn'} \tag{8}$$

and crack initiation occurs when D equals a unit.

The material parameters ϵ_f', σ_f, c, and n' in Eq. (8) depend on the specimen surface treatment and environmental conditions. Therefore, these parameters should be derived from

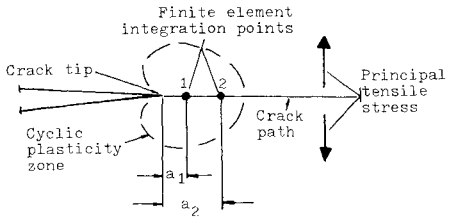

Fig. 3 Location of discrete points in front of crack tip for calculation of crack growth rate.

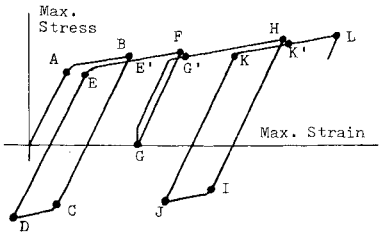

Fig. 4 Pair of reversals count.

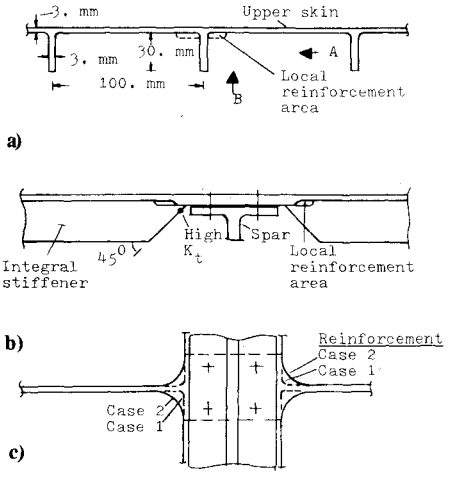

Fig. 5 Details of aircraft integral stiffened skin. a) Typical section. b) View A. c) View B.

uniaxial testing with the same conditions as exist in the real structure. The effect of temperature, loading frequency, and strain rate are not included in the present damage criterion. For a material with different tension-compression properties the values for n' and σ_f in Eq. (8) are changed according to the sign of the average mean stress $\bar{\sigma}_m$.

Cyclic plasticity causes relaxation of the mean stress at room temperature. Reference 14 shows that the rate of stress relaxation decreases exponentially with the number of cycles as a function of the plastic strain amplitude. Following this assumption, the original mean stress $\bar{\sigma}'_m$ relaxes to $\bar{\sigma}_m$ after $2N$ reversals, as follows[11]:

$$\bar{\sigma}_m = \bar{\sigma}'_m (2N)^{-r(\int d\epsilon^p/2)} \tag{9}$$

where r is a material parameter related to ϵ'_f. In Ref. 11, a value of r of 277 has been assumed for aluminum alloy 7075-T6 plate. This r value causes relaxation of the existing mean stress down to 0.01% of its initially computed value within two fully reversed plastic strain cycles of an amplitude of $0.1\epsilon'_f$. The mean stress value $\bar{\sigma}_m$ from Eq. (9) is substituted into Eq. (8).

Crack Growth Rate Criterion

It has been shown that a strong correspondence exists between Coffin-Manson formula and crack growth rate.[15,16] In the present paper the damage accumulation formulation [Eq. (8)] for crack initiation is also applied for crack growth prediction.

The cumulative damage is computed by Eq. (8) at two discrete points which are located just in front of the crack tip. These discrete points are defined by two integration points of the finite element adjacent to the crack tip. Figure 3 designates these integration points as 1 and 2; they are located at distances of a_1 and a_2 from the crack tip, respectively. Assume that the accumulated damage at points 1 and 2 is termed D_1 and D_2, respectively. If the crack propagates by the small distance of $(a_2 - a_1)$, the damage at point 2 becomes D_1; thus, the average cumulative damage value is $\frac{1}{2}(D_1 + D_2)$. The crack growth rate, $da/d(2N)$, is approximated as follows[11]:

$$\frac{da}{d(2N)} = \frac{a_2 - a_1}{[2/(D_1 + D_2) - 1/D_1]} \tag{10}$$

where a is the half length of the existing crack. Equation (10) indicates that a complete fracture occurs when $D_2 \geq D_1$.

The finite-element integration points, whose cumulative damage values are used for the crack growth rate prediction, are chosen according to the predicted crack path, which is usually normal to the direction of the principal tensile stress. These integration points should be well within the material's cyclic plasticity range. This requires a reasonably small finite element to be used at the crack tip.

When several analyses with different crack size are performed, it is assumed that the residual stresses from the previous analysis have been relaxed to zero. However, the damage values are continuously accumulated for all the integration points of the finite elements, such that the whole damage accumulation process is history dependent.

Damage Accumulation Technique

The damage criterion in Eq. (8) is applied to each pair of reversals separately, and the results are accumulated during the entire applied loading history. Each pair of reversals is defined, as mentioned before, during two subsequent plastic unloadings made in reversal directions. The plastic unloadings in Fig. 4, for example, occur at points B, D, F, H, J, and L. However, the unloading at point F is not considered because the following plastic unloading at point H is not in the reversal direction. Therefore, the first pair reversal is AB-CD, the second pair reversal is EH-IJ, and so on.

The present damage accumulation technique does not account for the effect of elastic reversals, i.e., it ignores the effect of the elastic loop FGG' in Fig. 4. This is justified because the damage criterion [Eq. (8)] employs the material's cyclic ductility strain ϵ'_f, which is smaller than the material's monotonic ductility strain. The technique does incorporate the cyclic parameters n' and c; thus, it is assumed that the fatigue damage is due mainly to the plasticity cycles.

Computer Program

The present approach has been programmed for computer usage as described in Ref. 17. This computer program utilizes the NONSAP program's two-dimensional isoparametric finite element and its numerical solution procedure.[18] The present cyclic plasticity model and damage accumulation criteria have been merged into the NONSAP program.

Illustrative Examples

A typical stiffened panel on aircraft wing is shown in Fig. 5. The integral stiffeners' cross section, at the spar location, is changed as shown in Fig. 5b. Axial loads due to the overall wing bending could lead to high stress concentration at the indicated point. Generally, this can be significantly reduced by addition of a small local material area.[19] Two cases (1 and 2) of different amount of reinforcement areas are analyzed. Figure 6a shows the finite-element model used. Plane stress

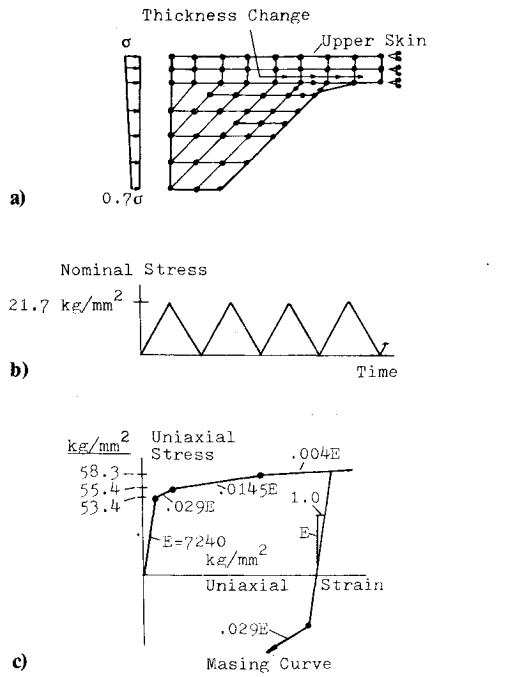

Fig. 6 Mathematical model for stiffened skin example. a) Finite-element model. b) Applied compressive loading. c) Material uniaxial curve.

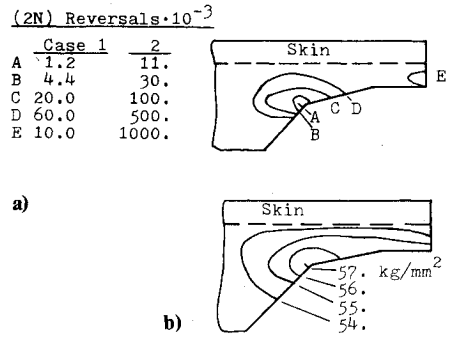

Fig. 7 Results for uncracked stiffened skin example. a) Equal damage curves indicating number of reversals to crack initiation. b) Maximum von Mises stress distributions.

isoparametric elements are employed. The applied load is compression which varies with the stiffener's depth, as shown. The applied load variation with time, shown in Fig. 6b, causes local compressive yielding (maximum elastic stress concentration equals 2.7) and high residual tensile stresses after unloading. Therefore, although no tensile loads are applied, a cyclic compression-tension stress state exists, causing crack initiation and crack propagation. The material's uniaxial stress-strain curve is idealized by piecewise linear segments, as shown in Fig. 6c. The material's fatigue properties are based on constant strain amplitude testing data from Ref. 20. The fatigue strength parameter σ_f' is assumed to be equal to the monotonic fracture strength σ_f which equals 75.9 kg/mm^2. The engineering ultimate stress, for comparison, is 59.0 kg/mm^2. The fatigue ductility parameter ϵ_f' is assumed to be 0.18, while the measured monotonic fracture ductility ϵ_f equals 0.41. The Coffin-Manson exponent c is estimated to be -0.52. The cyclic uniaxial exponent n' is shown[20] to be 0.11, while the monotonic uniaxial exponent n equals 0.113. Specification of stress relaxation exponent r is not required for the present examples because the resulting mean stresses are negligible.

Figure 7a shows computed damage curves for the uncracked structural component. Each curve indicates an equal

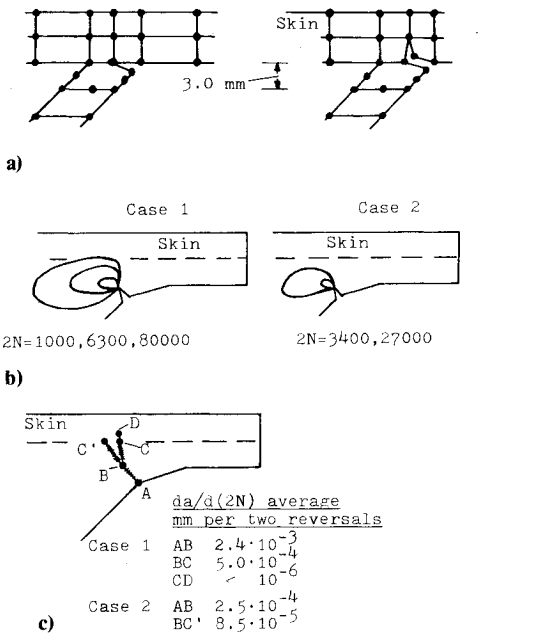

Fig. 8 Results for cracked stiffened skin example. a) Modified finite-element models due to crack growth. b) Equal damage curves distributions. c) Crack growth rate and orientation.

damage accumulation value. Crack initiation occurs at point A after 1200 reversals for case 1 and 11,000 reversals for case 2. So the small reinforcement area, shown in Fig. 5 as case 2, significantly improves the life to crack initiation. Figure 7b shows von Mises equivalent stress distribution for case 1. It is apparent that the stress gradient is much smoother than the damage gradient. The latter is based mainly on the plastic strain. This demonstrates the inability of stresses to predict the fatigue failure in a plastic field.

Figure 8a shows examples of the cracked finite-element models. The left-hand model represents the initial crack path. The initial crack is oriented almost perpendicular to the component's free edge (and to the principal tensile stress). However, in order to maintain the element's parallelogram shape—an important factor for numerical accuracy—the crack's direction is changed slightly as shown. It is judged that for this particular case the stress-strain variation will not be influenced. The right-hand model in Fig. 8a represents the progressive crack growth. Equal damage curves before the crack changes its direction are shown in Fig. 8b. Crack growth rate values along the crack path are derived from the curves shown in Figs. 7a and 8b by employing Eq. (10). The results are summarized in Fig. 8c. For case 1, after crack initiation the average growth rate is 0.0024 mm per pair of reversal. Then the crack growth rate slows to 0.0005 mm, and also changes direction from point B in Fig. 8c. Similar behavior is also indicated for case 2, but in this case the crack path is different because of the local additional reinforcement area.

Conclusion

The present analytical procedure combines the finite-element method and cyclic plasticity theory with damage accumulation criteria for prediction of both life to crack initiation and crack growth rate in a cyclic plasticity field. The present procedure accounts for the following:

1) The effects of residual stresses and multiaxial stress redistributions at the crack tip which lead to crack growth retardation. The effect of possible crack closure is not directly incorporated. However, this phenomenon is approximated by including the effect of residual compressive stresses, the main cause of crack closure.

2) The effects of multiple overloads, negative loads, and varying load spectra.

3) The effects of the interaction of close cracks, interaction of the skin and the stiffener, and any complex geometry that can be idealized by the finite-element method.

The required input data include the loading spectrum, the material's cyclic uniaxial stress-strain curve, the material's cyclic stress-plastic strain exponent, and the Coffin-Manson low-cycle fatigue parameters. These parameters are derived only from smooth uniaxial specimens. The method also requires the material's stress relaxation exponent.

The life to crack initiation and the crack growth rate are evaluated from results of each finite-element model separately. The damage values are accumulated through the subsequent models which represent the changing crack length. Residual stresses from the previous cracked finite-element models are assumed to relax to zero.

The damage criterion used for crack growth rate and, to some extent, the criterion for crack initiation are novel and without sound experimental supporting evidence. However, it is believed that, in combination with engineering judgment, they can be used to obtain useful qualitative results.

References

[1] "Metallic Materials and Elements for Aerospace Vehicle Structures," MIL-HDBK-5C, Dec. 1978.

[2] "Damage Tolerant Design Handbook," Battelle Columbus Lab., MCIC-HB-01, Dec. 1972.

[3] Wood, H.A. and Eagle, R.M. Jr., "USAF Damage Tolerant Design Handbook: Guidelines for the Analysis and Design of Damage Tolerant Aircraft," AFFDL-TR-79-3021, March 1979.

[4] Mattos, R.J. and Lawrence, F.V., "Estimation of the Fatigue Crack Initiation Life in Welds Using Low Cyclic Fatigue Concepts," SAE SP-424, 1978.

[5] Socie, D.F., "Fatigue-Life Prediction Using Local Stress-Strain Concepts," *Experimental Mechanics*, Vol. 17, Feb. 1977, pp. 50-56.

[6] Mowbray, D.F. and McConnelee, J.E., "Application of Finite Element Stress Analysis and Stress-Strain Properties in Determining Notch Fatigue Specimen Deformation and Life," *Cyclic Stress-Strain Behavior-Analysis, Experimentation, and Failure Prediction*, ASTM STP-519, 1973, pp. 151-169.

[7] Morrow, J., "Cyclic Plastic Strain Energy and Fatigue of Metals," *Internal Friction, Damping and Cyclic Plasticity*, ASTM STP-378, 1965, pp. 45-87.

[8] Topper, T.H., Wetzel, R.M., and Morrow, J., "Neuber's Rule Applied to Fatigue of Notched Specimens," *Journal of Materials*, Vol. 4, March 1969, pp. 200-209.

[9] Ratwani, M.M. and Wilhem, D.P., "Development and Evaluation of Method for Plane Stress Fracture Analysis," AFFDL-TR-73-42, Aug. 1977.

[10] Dowling, N.E. and Begley, J.A., "Fatigue Crack Growth During Gross Plasticity and the J-Integral," *Mechanics of Crack Growth*, ASTM STP-590, 1976, pp. 82-103.

[11] Kalev, I., "Cyclic Plasticity Models and Application in Fatigue Analysis," *Computers and Structures*, Vol 13, 1981, pp. 709-716.

[12] Sandor, B.I., *Fundamentals of Cyclic Stress and Strain*, University of Wisconsin Press, Madison, 1972, pp. 85-112.

[13] Jhansale, H.R., "Evaluation of Deformation Phenomena of Materials for Fatigue Analysis," *Journal of Testing and Evaluation*, Vol. 3, Sept. 1975, pp. 348-354.

[14] Jhansale, H.R. and Topper, T.H., "Engineering Analysis of the Inelastic Stress Response of a Structural Metal Under Variable Cyclic Strains," *Cyclic Stress-Strain Behavior Analysis, Experimentation and Failure Prediction*, ASTM STP-519, 1973, pp. 246-270.

[15] Kaisand, L.R. and Mowbray, D.F., "Relationships Between Low-Cyclic Fatigue Crack Growth Rate Properties," *Journal of Testing and Evaluation*, Vol. 7, Sept. 1979, pp. 270-280.

[16] Majumdar, S. and Morrow, J., "Correlation Between Fatigue Crack Propagation and Low Cycle Fatigue Properties," *Fracture Toughness and Slow-Stable Cracking*, ASTM STP-559, 1974, pp. 159-182.

[17] Kalev, I., "A Computer Program for Cyclic Plasticity and Structural Fatigue Analysis," NASA CR-163101, Nov. 1980.

[18] Bathe, K.J., Wilson, E.L., and Iding, R., "NONSAP-Structural Analysis Program for Static and Dynamic Response of Nonlinear Systems," University of California, Berkeley, Rept. UC SESM 74-3, Feb. 1974.

[19] Impellizzeri, L.F., "Structural Fatigue Analysis and Testing for Fighter Aircraft," *Design against Fatigue*, AGARD CP-141, Dec. 1973.

[20] Endo, T. and Morrow, J., "Cyclic Stress-Strain and Fatigue Behavior of Representative Aircraft Metals," *Journal of Materials*, Vol. 4, March 1969, pp. 159-175.